Kinetics of Strain-Related Morphology Transformation in $YBa_2Cu_3O_{7-\delta}$

S. Semenovskaya and A. G. Khachaturyan
Department of Materials Science, Rutgers University, P.O. Box 909, Piscataway, New Jersey 08855-0909
(Received 6 February 1991)

The kinetics of ordering with a reduction of a crystal lattice point symmetry and related transformation-induced elastic strain is considered for the first time. Ordering in $YBa_2Cu_3O_{7-\delta}$ is specifically discussed. A computer simulation predicts a temporal development of the microstructure through the tweed to the (110) microtwin structure driven by the elastic strain accommodation. The results obtained are quite general in the sense that predicted morphologies are typical for other systems with the point-symmetry reduction where the elastic strain accommodation plays an important role.

PACS numbers: 74.70.Vy, 61.14.Hg

Any phase transformation reducing the crystal lattice point symmetry results in a misfit between the parent and product phases and between different orientation variants of the ordered phase (structure domains). An accommodation of the elastic strain induced by the misfit causes a structural instability of the single-domain state of the product phase with respect to the formation of a coherent mixture of its twin-related orientation variants [1,2]. This structural instability is similar to that producing domains in ferromagnets and ferroelectrics. The similarity is a result of a profound physical and mathematical analogy between the strain-induced and magnetostatic (electrostatic) dipole-dipole interactions between finite elements of a low-symmetry phase [2]. The elastic interaction, as any dipole-dipole–type interaction, modifies the classical Gibbs thermodynamics since the total bulk free energy becomes dependent on the shape, orientation, and mutual location of the phase components. A sum of the morphology-dependent energies, elastic and interfacial, is minimized by a morphology consisting of lamellae of alternating twin-related orientation variants of the low-symmetry phase (polysynthetic twins) which form macroscopic plates [1–3]. Typical examples of such transformations are fcc→bcc, cubic→tetragonal martensitic transformations, as well as any congruent ordering reaction resulting in a reduction of a point-group symmetry (for example, fcc CuAu→fct CuAu I). A good and important generic example of such an ordering system is the high-temperature superconducting oxide $YBa_2Cu_3O_{7-\delta}$ undergoing a tetragonal→orthorhombic transition.

The stable twinned morphology does not necessarily form at once. We may always expect an occurrence of intermediate transient states and, particularly, so-called tweed structure along the transformation path [4–6]. It is generally believed that the tweed pattern is associated with the transformation strain, but, to our knowledge, there is no theory where the kinetic mechanism of the formation of tweed and twin patterns in an ordering system would be investigated and there is very little known about the structure and morphology of transient states in general. The purpose of this work is an investigation of a transformation path during ordering in $YBa_2Cu_3O_{7-\delta}$ by a computer-simulation technique.

Oxygen ordering of a second kind in $YBa_2Cu_3O_{7-\delta}$ is caused by a redistribution of oxygen atoms over interstitial sites in basal (001) Cu-O planes separated by three perovskite unit cells. The positions of interstitial sites in (001) basal Cu-O planes are shown in Fig. 1(a). Each interstitial site in the $a\times a\times 3a$ lattice is characterized by a translation vector $\mathbf{r}$ that designates a Cu atom, nearest to the relevant interstitial site, and by a distance $\mathbf{h}_p$ between this site and the Cu atom [$\mathbf{h}_1=a(\frac{1}{2}00)$, $\mathbf{h}_2=a(0\frac{1}{2}0)$, where the index p labels the sublattices, $p=1,2$]. An O-atom distribution is characterized by occupation probabilities $c_p(\mathbf{r},t)$ to find an O atom in a site $(p,\mathbf{r})$ at the time t. This distribution is defined on the time-dependent ensemble. In a disordered tetragonal (T) phase O atoms are randomly distributed over interstitial sites of both interstitial sublattices, and thus, $c_p(\mathbf{r},t)=\bar{c}$, where $\bar{c}$ is the fraction of interstitial sites occupied by O

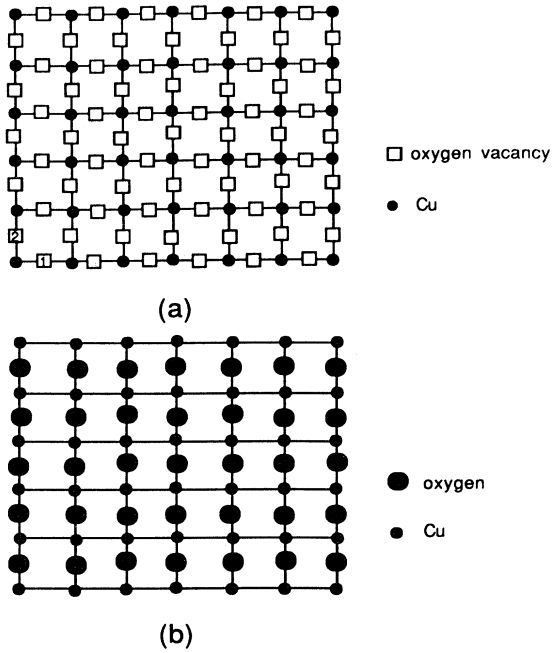

FIG. 1. (a) Positions of interstitial sites (oxygen vacancies) in (001) basal planes. (b) Orthorhombic completely ordered phase.

atoms. Ordering results in a preferential occupation of one of the sublattices caused by a transfer of O atoms from one interstitial sublattice to another. The completely ordered distribution in a basal (001) plane is shown in Fig. 1(b). The ordered phase is orthorhombic (O phase). The $T \rightarrow O$ reduction of the symmetry results in an orthorhombic distortion and, thus, generates the elastic strain.

The diffusional kinetics of ordering can be described by a microscopic crystal lattice site diffusion equation [2,7]:

$$\frac{dc_p(\mathbf{r},t)}{dt} = \sum_{q=1}^{q=2} \sum_{\mathbf{r}'} L(\mathbf{r}-\mathbf{r}')_{pq} \frac{\delta F}{\delta c_q(\mathbf{r}',t)} , \qquad (1)$$

where F is the free-energy functional of the distribution function $c_p(\mathbf{r},t)$, and $L(\mathbf{r}-\mathbf{r}')_{pq}$ is a matrix of kinetic coefficients characterizing the probability of an elementary diffusional jump from the site $(q,\mathbf{r}')$ to the site $(p,\mathbf{r})$ during a time unit. The summation over $\mathbf{r}'$ is carried out over all N unit cells of a crystal. Equations (1) are, actually, Onsager equations with respect to $2N$ relaxing parameters $c_p(\mathbf{r},t)$, where the variational derivative, $\delta F/\delta c_q(\mathbf{r}',t)$, is a thermodynamic driving force.

As in most ceramic oxides, the oxygen-oxygen interaction in $YBa_2Cu_3O_{7-\delta}$ is long range [8–10]. The free energy F, entering Eq. (1), includes the strain energy induced by interstitial oxygen. The strain-induced interaction is also long range [2]. As is known, the mean-field free energy is a good approximation for a long-range interaction, especially in the presence of the strain-induced interaction [11]. The approximation, however, also becomes asymptotically correct irrespective of the interaction radius if the long-range order parameter is large [12]. Using the mean-field approximation for the free energy [2],

$$F = \tfrac{1}{2} \sum_{pq\mathbf{r}\mathbf{r}'} \overline{W}(\mathbf{r}-\mathbf{r}')_{pq} c_p(\mathbf{r}) c_q(\mathbf{r}') + k_B T \sum_{p\mathbf{r}} \{c_p(\mathbf{r}) \ln c_p(\mathbf{r}) + [1-c_p(\mathbf{r})] \ln[1-c_p(\mathbf{r})]\} ,$$

where $\overline{W}(\mathbf{r}-\mathbf{r}')_{pq}$ is a pairwise interaction energy between oxygen atoms in sites $(p,\mathbf{r})$ and $(q,\mathbf{r}')$ that includes a strain-induced interaction, k_B is the Boltzmann constant, and T is the temperature, we can present the Fourier transform of (1) in the form

$$\frac{d\tilde{c}_p(\mathbf{k},t)}{dt} = \sum_{q=1}^{q=2} \sum_{s=1}^{s=2} \tilde{L}(\mathbf{k})_{pq} \left[[V(\mathbf{k})_{qs} + B(k)_{qs}] \tilde{c}_p(\mathbf{k},t) + \delta_{qs} k_B T \left(\ln \frac{c_s(\mathbf{r},t)}{1-c_s(\mathbf{r},t)} \right)_{\mathbf{k}} \right] , \qquad (2)$$

where δ_{qs} is a Kronecker symbol, $\tilde{c}_p(\mathbf{k},t)$, $V(\mathbf{k})_{qs}$, $\tilde{L}(\mathbf{k})_{pq}$, and $(\ln c_s(\mathbf{r},t)/[1-c_s(\mathbf{r},t)])_{\mathbf{k}}$ are Fourier transforms of the respective functions, $c_p(\mathbf{r},t)$, $W(\mathbf{r})_{qs}$, $L(\mathbf{r})_{pq}$, and $\ln c_s(\mathbf{r},t)/[1-c_s(\mathbf{r},t)]$. $W(\mathbf{r})_{qs}$ is a pairwise interaction that does not include the strain-induced interaction, $\mathbf{k}$ is a wave vector within the first Brillouin zone of the disordered tetragonal phase, and $B(\mathbf{k})_{qs}$ is the Fourier transform of a pairwise strain-induced O-O interaction potential.

Since the $T \rightarrow O$ ordering in $YBa_2Cu_3O_{7-\delta}$ is induced by the antisymmetric irreducible representation of the space group related to the vector $\mathbf{k}=0$, a long-wave approximation for the function $B(\mathbf{k})_{pq}$ can be used:

$$B(\mathbf{k})_{pq} \approx -v n_i \sigma(p)_{ij} \Omega(\mathbf{k})_{jk} \sigma(q)_{kl} n_l , \qquad (3)$$

where $\sigma(p)_{ij} = c_{ijkl} \varepsilon(p)^{O}_{kl}$, $\varepsilon(p)^{O}_{kl}$ is the concentrational coefficient of a crystal lattice expansion associated with O atoms in the pth interstitial sublattice, c_{ijkl} is the elastic strain modulus tensor, v is the unit-cell volume, $\Omega(\mathbf{k})_{ij}$ is the Green tensor reciprocal to $c_{ijkl} n_j n_k$, and $\mathbf{n} = \mathbf{k}/k$ [2,13].

Assuming an elementary diffusion jump only between nearest-neighbor sites, we obtain the Fourier transform

$$\tilde{L}(\mathbf{k})_{pq} = 4L_1 \begin{pmatrix} -1 & \cos\mathbf{k}\cdot\mathbf{h}_1 \cos\mathbf{k}\cdot\mathbf{h}_2 \exp[i\mathbf{k}\cdot(\mathbf{h}_1-\mathbf{h}_2)] \\ \cos\mathbf{k}\cdot\mathbf{h}_1 \cos\mathbf{k}\cdot\mathbf{h}_2 \exp[-ik\cdot(h_1-h_2)] & -1 \end{pmatrix} ,$$

where $L_1 = 1/\tau$, and τ is a characteristic time of an elementary jump. Equation (2) is reduced to the Cahn-Hilliard equation in the long-wave limit in the Bravais-lattice case [14]. A set of $2N$ nonlinear kinetic equations (2) with the periodic boundary condition is solved numerically by the Euler method. The solution $c_p(\mathbf{r},t)$ completely describes the ordering and morphology transformations.

Since the Cu-O basal (001) planes shown in Fig. 1 are separated by three perovskite unit cells, we may use a two-dimensional ordering model for our computer simulation as a first approximation; $N = 128 \times 128$. The strain tensors in (3) are $\varepsilon(1)^{O}_{ij} = -\varepsilon(2)^{O}_{ij} = \varepsilon_0 \begin{pmatrix} 1 & 0 \\ 0 & -1 \end{pmatrix}$ where according to the experimental data [15], $\varepsilon_0 \approx 0.01$, $a \approx 3.856$ Å, $v = 173$ Å^3. The elastic constants c_{ijkl} for $YBa_2Cu_3O_{7-\delta}$ are estimated in [9]. We have chosen the values $c_{11} = 3.9 \times 10^{12}$ dyn/cm^2, $c_{12} = 1.36 \times 10^{12}$ dyn/cm^2, and $c_{44} = 0.91 \times 10^{12}$ dyn/cm^2.

For $W(\mathbf{r})_{pq}$ we have chosen the anisotropic screened Coulomb potential proposed by Aligia, Garces, and Bondaleo [16] with anisotropy for the next-nearest-neighbor pairs. The anisotropy is introduced by a multiplier, $1 \pm f$, with the minus sign for an interaction across a Cu atom and the plus sign otherwise; $f = 0.6$ is used. The fact of observation of the $2a \times a$ ordered phase in nonstoichiometric oxides indicates that the O-O interaction has a range not less than $2a$. We chose the screening radius

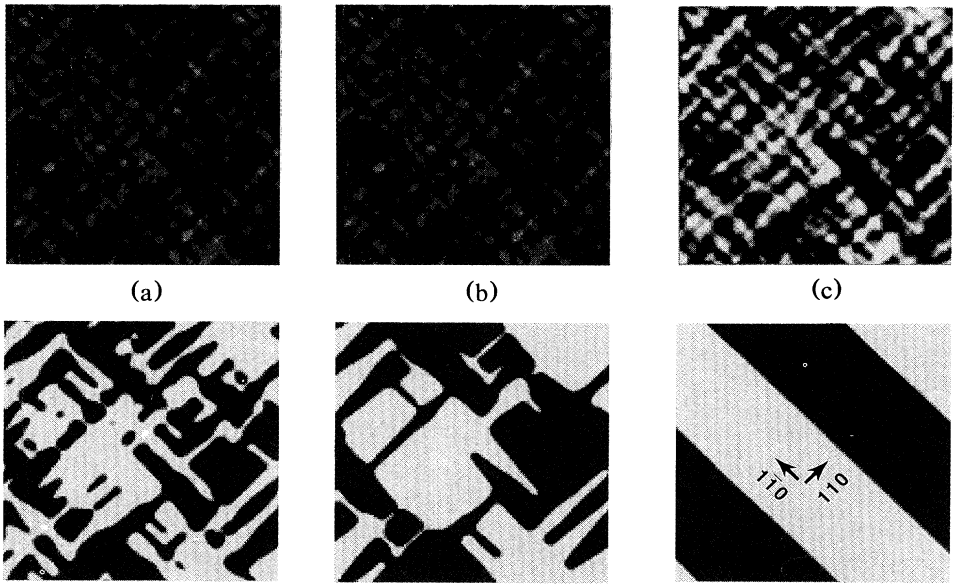

FIG. 2. Simulated transient structures along the transformation path from an initial disordered state to the (110) twinned ordered state as a function of the reduced time t^*: (a) $t^*=1.24$, (b) $t^*=1.48$, (c) $t^*=2$, (d) $t^*=6$, (e) $t^*=24$, (f) $t^*=88$. (a)–(c) demonstrate the development of the tweed structure; (d)–(f) show the tweed → twin rearrangement.

$r_D=5a\sqrt{2}$ (our tests with the screening radii between $a/\sqrt{2}$ and $8a/\sqrt{2}$ gave, practically, the same results). The oxygen charge was chosen to be $z=0.13e$, where e is the electron charge. This potential is supplemented by a Born-Meyer repulsion correction δW_1 for the nearest-neighbor pairs, where $\delta W_1=0.945\times10^{13}$ erg. These numerical parameters for $W(\mathbf{r})_{pq}$ are chosen by fitting to the observed ordering temperatures $T\rightarrow O$ and $O\rightarrow O'$ at the stoichiometry $\delta=0.5$.

The ordering-related morphology transformations have been simulated by "quenching" a disordered T phase well below the order-disorder temperature T_0 (the reduced temperature $T^*=T/T_0=0.73$). The initial disordered state has been described by a function $c_p(\mathbf{r},0)$ randomly and "infinitesimally" fluctuating around $\bar{c}=0.5$. Computer-simulation results shown in Figs. 2(a)–2(f) demonstrate the temporal evolution of the microstructure characterized in these figures by a long-range order parameter $\eta(\mathbf{r},t)=c_1(\mathbf{r},t)-c_2(\mathbf{r},t)$. Regions with $\eta<0$ describe orientation domains of the first type (black) with preferred occupation of the first interstitial sublattice; regions with $\eta>0$ (light) characterize domains of the second type. The larger η is, the lighter is the color of a domain of the second type. Figure 3(a) gives a more detailed representation of the structure shown in Fig. 2(c). As follows from these results, the value of $\eta(\mathbf{r})$, close to equilibrium, is reached very quickly, during the reduced time $t^*=4t/\tau\sim1$.

Figures 2 and 3(a) demonstrate the appearance of a coherent mixture of ordered domains which are two orientation variants of the O phase. The domains are twin related with strongly pronounced (110) boundaries. Figures 2(a)–2(c) and 3(a) illustrate the development of the tweed structure aligned along the ⟨110⟩ directions. Figures 2(d) and 2(f) show how the tweed structure transforms into a (110) twin structure. Simulated strain-induced diffraction patterns of the structure shown in Figs. 2(c) and 3(a) are presented in Fig. 3(b). These diffraction patterns, typical for the tweed structure, are usually observed for phase transformations with a reduction of a point symmetry (see, for example, [4–6]). Both the striation along both ⟨110⟩ directions in structures and the ⟨110⟩ streaks on the diffraction patterns, followed from our simulation [Figs. 2(a)–2(c) and 3(b), respectively], have been observed on electron microscopic images and thoroughly studied by Zhu, Suenaga, and Moodenbaugh in $YBa_2(CuFe)_3O_{7-\delta}$ [17]. They have also been observed by Zhu, Suenaga, and Moodenbaugh [17] and by Van Tandeloo *et al.* [18] in $YBa_2Cu_3O_{7-\delta}$. Comparison of the electron microscopic pictures obtained by Zhu, Suenaga, and Moodenbaugh [17] (Fig. 4) and the computer-simulated pictures in Figs. 2(a)–2(c) shows excellent agreement. Our results are also in agreement with the kinetics recently observed in an electron microscope, shown in an *in situ* filmed movie by Van Tandeloo. The simulated kinetics demonstrate that the tweed structure is a transient state along the transformation path and that the tweed formation as well as the further tweed → twin rearrangement [Figs. 2(c)–2(f)] is driven by the elastic strain accommodation. The predicted ultimate (110) twin structure formed by two orientation variants of the O phase is also in agreement with electron

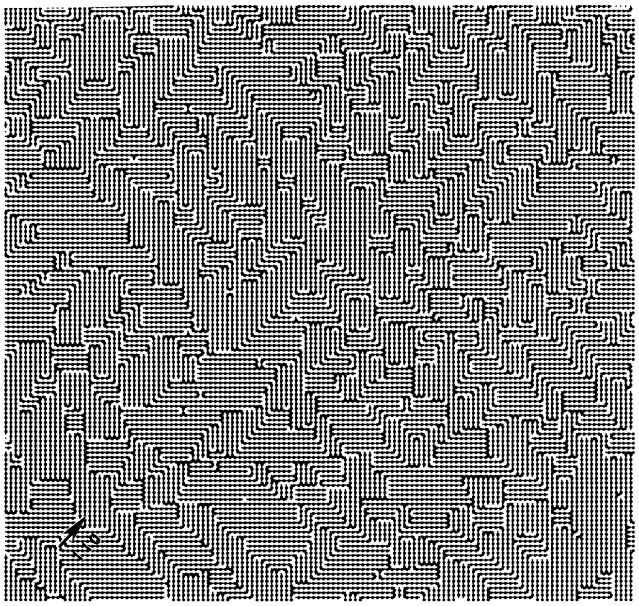

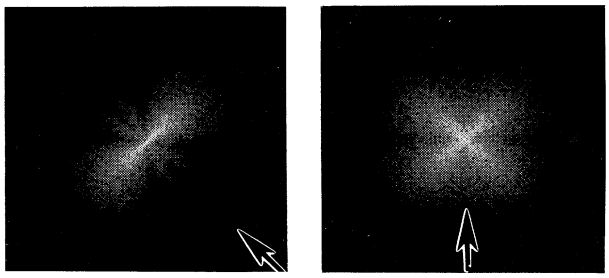

FIG. 3. (a) A "microscopic" representation of the tweed structure shown in Fig. 2(c) ($t^*=2$). The dots represent O atoms; Cu atoms (not resolved here) are located in between. (b) The simulated strain-induced diffuse scattering (logarithm of calculated intensity) around (220) and (400) reciprocal-lattice points from the tweed structure in (a) and Fig. 2(c). Arrows indicate the directions of the (220) and (400) reciprocal-lattice vectors.

microscopic observations.

It should be emphasized that the morphology transformation shown in Fig. 2 is mainly a result of the elastic strain accommodation. A sequence of structures along the transformation path is not sensitive to a model for a chemical free energy if the elastic strain contribution is properly taken into account. For example, the macroscopic phenomenological Ginzburg-Landau approximation for the chemical free energy leads to the same morphology transformations.

The authors gratefully acknowledge support from the Division of Materials Science, U.S. DOE, under Grant No. DE-FG05-90ER45430. Computer simulations were partially performed on the Cray-YMR computer at the Pittsburgh Supercomputer Center. We are grateful to

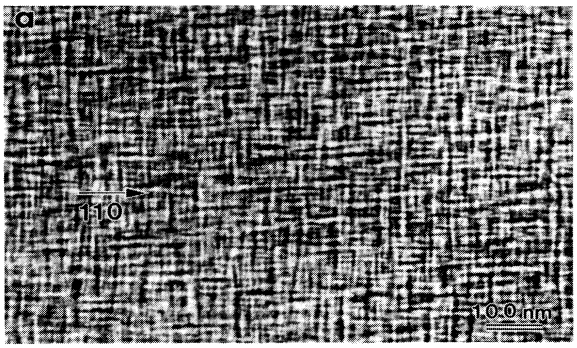

FIG. 4. Electron microscopic pictures of the tweed structure observed in $YBa_2(CuFe)_3O_{7-\delta}$ [17] (courtesy of Zhu, Suenaga, and Moodenbaugh).

Dr. Long-Qing Chen, Dr. Y. Zhu, and Yunzhi Wang for numerous discussions and help.

[1] A. G. Khachaturyan and G. A. Shatalov, Zh. Eksp. Teor. Fiz. **56**, 1037 (1969) [Sov. Phys. JETP **29**, 557 (1969)].
[2] A. G. Khachaturyan, *The Theory of Structural Transformation in Solids* (Wiley, New York, 1983).
[3] A. L. Roitburd, Fiz. Tverd. Tela (Leningrad) **10**, 3619 (1968) [Sov. Phys. Solid State **10**, 2870 (1969)].
[4] L. E. Tanner, Philos. Mag. **14**, 111 (1966).
[5] D. E. Laughlin, R. Sinclair, and L. Tanner, Scr. Metall. **14**, 373 (1980).
[6] I. M. Robertson and C. M. Wayman, Philos. Mag. A **48**, 443 (1983).
[7] A. G. Khachaturyan, Fiz. Tverd. Tela (Leningrad) **9**, 2595 (1967) [Sov. Phys. Solid State **9**, 2040 (1968)].
[8] A. M. Stoneham and J. H. Harding, Annu. Rev. Phys. Chem. **37**, 53 (1986); in *Computer Simulation of Solids,* edited by C. R. A. Catlow and W. C. Mackrodt, Series Lecture Notes in Physics Vol. 166 (Springer-Verlag, New York, 1982).
[9] R. C. Baetzold, Phys. Rev. B **38**, 11 304 (1988).
[10] S. Valkealahty and D. O. Welch, Physica (Amsterdam) **162–164C**, 540 (1989).
[11] V. G. Vaks, A. I. Larkin, and S. A. Pikin, Zh. Eksp. Teor. Fiz. **51**, 361 (1966) [Sov. Phys. JETP **24**, 240 (1966)].
[12] R. A. Suris, Fiz. Tverd. Tela (Leningrad) **4**, 1154 (1962) [Sov. Phys. Solid State **4**, 850 (1962)].
[13] A. G. Khachaturyan, Fiz. Tverd. Tela (Leningrad) **9**, 2861 (1967) [Sov. Phys. Solid State **9**, 2249 (1968)].
[14] J. W. Cahn and J. E. Hilliard, J. Chem. Phys. **31**, 688 (1959).
[15] R. J. Cava, B. Batlogg, C. H. Chen, E. A. Rietman, S. M. Zahurak, and D. Werder, Nature (London) **329**, 423 (1987).
[16] A. A. Aligia, J. Garces, and H. Bondaleo, Phys. Rev. B **42**, 10226 (1990).
[17] Yimey Zhu, M. Suenaga, and A. R. Moodenbaugh, Philos. Mag. **62**, 51 (1990).
[18] G. Van Tandeloo, D. Broddin, H. W. Zanderbergen, and S. Amelinckx, Physica (Amsterdam) **167C**, 627 (1990).

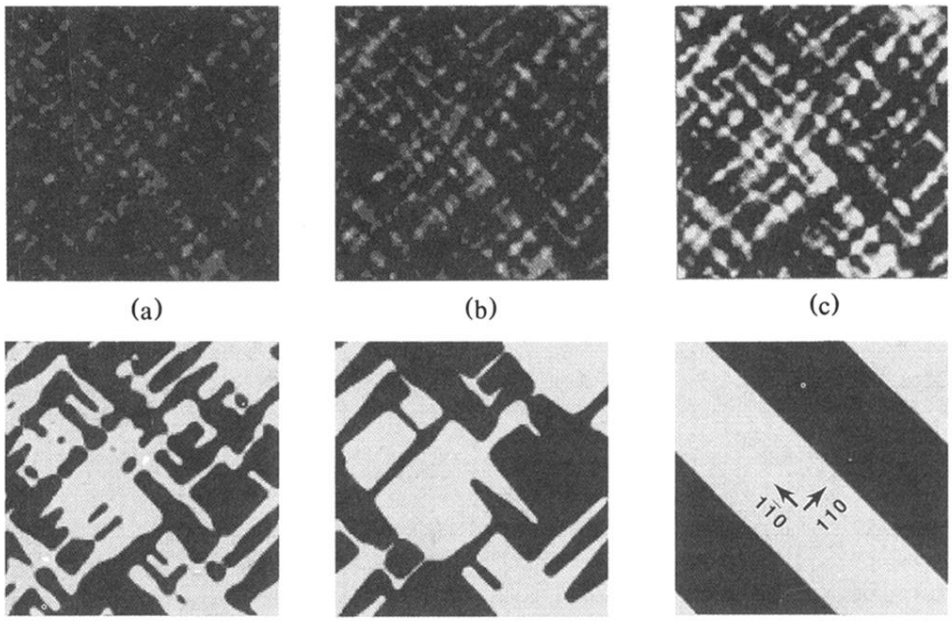

FIG. 2. Simulated transient structures along the transformation path from an initial disordered state to the (110) twinned ordered state as a function of the reduced time t^*: (a) $t^*=1.24$, (b) $t^*=1.48$, (c) $t^*=2$, (d) $t^*=6$, (e) $t^*=24$, (f) $t^*=88$. (a)–(c) demonstrate the development of the tweed structure; (d)–(f) show the tweed → twin rearrangement.

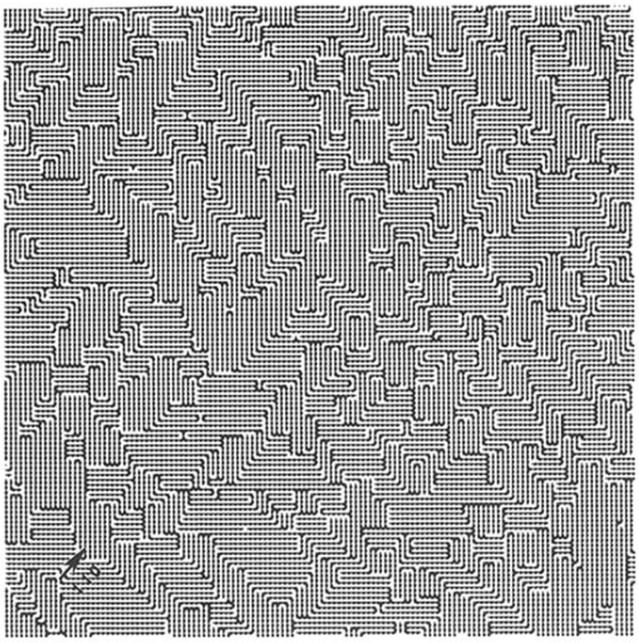

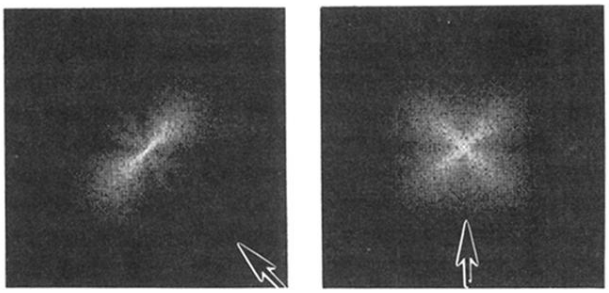

220 400

FIG. 3. (a) A "microscopic" representation of the tweed structure shown in Fig. 2(c) ($t^* = 2$). The dots represent O atoms; Cu atoms (not resolved here) are located in between. (b) The simulated strain-induced diffuse scattering (logarithm of calculated intensity) around (220) and (400) reciprocal-lattice points from the tweed structure in (a) and Fig. 2(c). Arrows indicate the directions of the (220) and (400) reciprocal-lattice vectors.

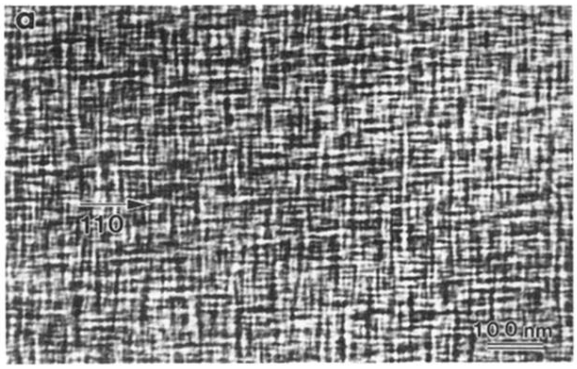

FIG. 4. Electron microscopic pictures of the tweed structure observed in $YBa_2(CuFe)_3O_{7-\delta}$ [17] (courtesy of Zhu, Suenaga, and Moodenbaugh).